Dynamic screening effects in x-ray absorption spectra

A. L. Ankudinov, A. I. Nesvizhskii,* and J. J. Rehr
Department of Physics, Box 351560, University of Washington, Seattle, Washington 98195
(Received 2 December 2002; published 21 March 2003)

Calculations of x-ray absorption for soft x rays are often dependent on screening of the x-ray field and the photoelectron–core-hole interaction. Though screening is usually calculated with static screening models, we find that *L*-shell x-ray absorption in 3*d* transition metals is sensitive to dynamic screening effects. This screened interaction is calculated here using a generalization of the time-dependent local-density approximation, based in part on the Bethe-Salpeter equation. For computational efficiency, our approach uses a local screening approximation based on a projection onto a local atomic basis. The approach yields efficient calculations of the spectra in terms of screened transition matrix elements, and can be implemented straightforwardly within a real-space Green's-function approach. Calculations for rare-gas solids demonstrate the effectiveness of this local model, and also give reasonable agreement with the observed fine structure. Calculations based on a dynamic-screening model account for the observed deviations of the L_3/L_2 intensity branching ratio from the 2:1 value of independent-electron theory.

DOI: 10.1103/PhysRevB.67.115120 PACS number(s): 78.70.Dm, 75.50.Cc, 78.20.Ls

I. INTRODUCTION

The independent-electron approximation is generally successful in describing near-edge x-ray-absorption spectra (XAS).[1] Indeed, many current calculations of XAS are based on an independent, quasiparticle approximation, with final-state potentials that include a core hole and inelastic losses. However, this independent-electron approximation can fail dramatically for soft x-ray edges, e.g., for rare gases[2] and for the $L_{2,3}$ edges of transition metals.[3–6] For atomic Xe, for example, this approximation yields x-ray-absorption cross sections which are much too large and shifted too low in energy. For $L_{2,3}$ XAS, the independent-electron approximation predicts an L_3/L_2 transition intensity ''branching ratio'' close to 2:1, while the observed ratio (Fig. 1) varies considerably with atomic number *Z*, and is closer to 1:1 for metals like Ti and V with nearly empty *d* bands.[7–9]

A number of approaches for understanding the observed failures of the independent-electron approximation have been proposed. These methods differ depending on how the Coulomb interactions between interacting electrons are handled. For example, the trends in the ''anomalous'' branching ratio vs atomic number *Z* have been calculated using atomic models, e.g., configuration interaction[4] (CI) and multiplets.[5] Physical explanations have been given based on models with spin-orbit and core-hole interactions plus ligand-field couplings.[5] An alternative approach, originally designed for atomic systems, makes use of the time-dependent local-density approximation (TDLDA).[2] The TDLDA yields a physical interpretation for the observed change in the cross sections in terms of screening of the x-ray field, and can also simplify the calculations.[2,10,11] For example, the TDLDA has been shown to give corrections to the independent particle approximation, which lead to remarkable agreement with experiment for x-ray absorption by rare gases.[2] Despite their formal differences, the results of these methods should in principle be comparable. For example, an exact CI calculation should give the same cross section as a TDLDA response function calculation, assuming that the exact exchange-correlation functional is known.

On the other hand, all atomic approaches ignore the detailed fine structure in the continuum due to multiple scattering from the environment of an absorbing atom in a material,[1] and hence are not fully appropriate for solids. Generalizations of the TDLDA for extended systems have also been developed.[11,12,6] In particular, an approach for *L*-edge XAS makes use of relativistic band-structure calculations.[6] These TDLDA approaches generally make use of static screening approximations. Though such static approximations are appropriate in the optical regime,[11,12] they are questionable at x-ray energies.

Our goal in this work is to achieve a quantitative understanding of such corrections to the independent-electron approximation based on generalizations of the TDLDA. One of our main purposes is to develop approximations which take into account the frequency dependence of the screening; that is, we aim to go beyond conventional implementations of the TDLDA with static screening models. Moreover, we aim to develop efficient algorithms for practical calculations in solids. To this end, we introduce a local approximation for the

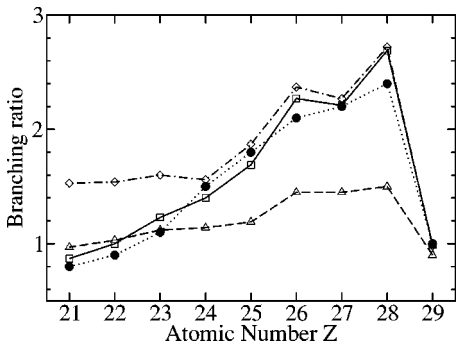

FIG. 1. L_3/L_2 intensity branching ratio for the transition-metal series, as defined in Ref. 6, from experiment (solid circles), and as calculated with different exchange-correlation kernels: RPA (triangles), adiabatic f_{xc}^0 (diamonds); and the dynamic model of this work (see text) $\tilde{f}_{xc}(\tilde{\omega})$ (squares).

screening based on an expansion in a local atomic basis. Thus our approach aims to treat screening at the atomic level. Moreover, we employ a representation of the TDLDA which permits the separation of the x-ray-absorption spectrum into contributions from the absorbing atom (i.e., the screened transition matrix elements which control the production of the photoelectron) and from propagation and scattering in the extra-atomic environment (i.e., the one-particle Green's function or propagator).

Our primary application is to deep-core XAS at soft-x-ray energies, e.g., the L edges of $3d$ transition metals. However, the approach is more general and can straightforwardly be applied to many other cases. Thus we have also carried out calculations for rare-gas atoms and solids. Our results for Xe, for example, are consistent with those of Ref. 2, but also include the extended fine structure for solid Xe. For $L_{2,3}$ XAS of $3d$ transition metals, we show that the observed branching ratio depends not only on dynamic screening of the x-ray field, but also on dynamic screening of the photoelectron–core-hole interaction.

II. MANY-BODY EFFECTS AND SCREENING IN XAS

The $L_{2,3}$ x-ray-absorption spectrum in solids corresponds to transitions from the $2p_{1/2}$ and $2p_{3/2}$ levels to continuum s and d states. Spin-orbit effects are thus essential to an adequate description.[4,5] In this work, spin orbit is included naturally within a Dirac-relativistic treatment, both in the initial and final states. Several many-body effects can be identified which contribute to a nonconstant L_3/L_2 intensity branching ratio.

(i) Inelastic losses: these can be represented in terms of lifetime and self-energy effects in independent-electron calculations. The lifetimes are different for the L_2 and L_3 edges due to the Coster-Kronig mechanism,[13] but this difference only increases the branching ratios, e.g., to about 3:1.

(ii) Dynamic core polarization: that is, the creation of local fields which screen the external x-ray field. This polarization effect may be treated[2,6] within the TDLDA by neglecting exchange terms, an approximation often referred to as the random-phase approximation (RPA). This leads to a considerable reduction of the branching ratio, but does not account well for its variation with Z, as shown in Fig. 1.

(iii) Screening of the photoelectron–core-hole interaction: this effect, which we find to be crucial, can be addressed in terms of a frequency-dependent exchange-correlation kernel $f_{xc}(\omega)$ in the TDLDA,[10] or a nonlocal, dynamically screened Coulomb $W(\omega)$ interaction within the Bethe-Salpeter equation (BSE).[14–18]

While a conventional TDLDA with static screening roughly explains the trends in the observed $L_{2,3}$ x-ray-absorption spectrum intensity branching ratios (Fig. 1), significant discrepancies remain compared to experiment for low -d occupation numbers (e.g., V and Ti). Going beyond the TDLDA generally requires a two-particle Green's function, i.e., the BSE. However, the generally nonlocal, dynamically screened Coulomb interaction between the core hole and photoelectron is usually difficult to calculate.

The importance of dynamic screening of the core hole in XAS is at first surprising, since it has been argued that corrections to the RPA are small,[2,6] or that an adiabatic kernel f_{xc}^0 or static screening within the BSE is adequate.[14,18] However, we show below that the inclusion of frequency dependence is well motivated for the problem of $L_{2,3}$ XAS of transition metals.

III. THEORETICAL APPROACH

A. The TDLDA

The TDLDA[2,6,10,11] provides an efficient formalism for calculations of response functions, including corrections to the independent-electron approximation. In particular, the approach avoids the complications of nonlocality in the time-dependent Hartree-Fock (TDHF),[19] BSE, or configuration-interaction techniques. However, its accuracy is limited by a lack of a precisely known exchange-correlation kernel $f_{xc}(\omega)$, as discussed below. The TDLDA was originally introduced for atoms,[2] but has since been extended to condensed systems.[11,6] The TDLDA and TDHF equations are closely similar to the BSE,[14–18] which provides a systematic many-body framework based on the two-particle Green's function for treating optical response. The main difference between the TDLDA and the BSE lies in the structure of $f_{xc}(\omega)$. In addition, the single-particle states in the BSE are quasiparticle states which take the electron and hole self-energies into account. Like the BSE, our approach also makes a quasiparticle approximation for single-particle states, with inelastic losses treated by a Hedin-Lundqvist electron-gas self-energy.[20] Such losses are crucial to quantitative calculations of XAS,[1] and also represent a dynamic-screening effect on the photoelectron state. Important in our approach is the use of a projection onto a local atomic basis and a real-space multiple-scattering (RSMS) formalism.[21] This local basis approach yields an efficient matrix formulation, yet retains much of the simplicity of the TDLDA, and gives reasonable agreement with experiment for the systems considered here. Local basis set methods have also been applied in various related calculations.[22,23] Improvements to the TDLDA based on the BSE have also been developed recently for optical spectra.[18]

Within the TDLDA (Ref. 2) or TDHF,[19] the x-ray-absorption spectrum (or cross section) $\sigma(\omega)$ can be expressed as an integral over the noninteracting response function $\chi_0(\vec{r},\vec{r},'\omega)$ and the screened x-ray field $\phi(\vec{r},\omega)$,

$$\sigma(\omega) = -\frac{4\pi\omega}{c}\int\int d^3r\,d^3r'\,\phi^*(\omega,\vec{r}) \times[\mathrm{Im}\,\chi_0(\omega,\vec{r},\vec{r}')]\phi(\omega,\vec{r}'),$$
$$\chi_0(\vec{r},\vec{r},'\omega) = \sum_{ij}(f_i - f_j)\frac{\psi_i^*(\vec{r})\psi_i(\vec{r}')\psi_j^*(\vec{r}')\psi_j(\vec{r})}{\omega + E_i - E_j + i0^+}. \quad (1)$$

Here f_i are Fermi occupation numbers (1 or 0 at zero temperature), and the sums run over all one-electron eigenstates $\psi_i(\vec{r})$ of the ground-state Hamiltonian. For notational simplicity, it is convenient to regard the continuous coordinates

$\vec{r}$ and $\vec{r}'$ as vector or matrix indices, which may be suppressed unless needed for clarity.

We stress that Eq. (1) is equivalent to an expression with ϕ replaced by the external x-ray field ϕ^{ext}, and χ_0 by the full response function $\chi=(1-\chi^0K)^{-1}\chi^0(\omega)$.[2] Thus an exact TDLDA treatment would yield an exact many-body cross section. The field $\phi(\omega)$ consists of the external field $\phi^{ext} \equiv \hat{\epsilon}\cdot\vec{r}$ (in the dipole approximation) plus an induced local field, given in matrix form by

$$\phi(\omega)=\epsilon^{-1}(\omega)\phi^{ext}(\omega), \quad \epsilon(\omega)=1-K(\omega)\chi^0(\omega). \quad (2)$$

Here $K(\vec{r},\vec{r},'\omega)$ denotes the particle-hole interaction (or TDLDA kernel), which contains direct and exchange parts, i.e.,

$$K(\vec{r},\vec{r},'\omega)=V(\vec{r},\vec{r}')+f_{xc}(\vec{r},\vec{r},'\omega), \quad (3)$$

where $V=1/|\vec{r}-\vec{r}'|$ is the Coulomb interaction, and $f_{xc}(\vec{r},\vec{r},'\omega)$ is the dynamic exchange-correlation contribution.

B. The TDLDA kernel $K(\omega)$

The exchange-correlation operator $f_{xc}(\vec{r},\vec{r},'\omega)$ in the TDLDA kernel is opposite in sign and partially cancels the effect of the Coulomb interaction V. In this paper, we consider several approximations for $f_{xc}(\omega)$ which is generally nonlocal and frequency dependent.

(i) The RPA ($f_{xc}=0$): to the extent exchange can be neglected, the RPA is adequate.[6]

(ii) Adiabatic TDLDA [$f_{xc}(0)=f^0_{xc}$]: this static limit $f^0_{xc}(\vec{r},\vec{r}')=\delta(\vec{r}-\vec{r}')\,\delta v_{xc}[\rho(\vec{r})]/\delta\rho$ avoids the nonlocality of the TDHF and is obtained from the ground-state LDA exchange-correlation potential $v_{xc}[\rho]$.

(iii) Dynamic TDLDA model: An LDA for the frequency dependence of $f_{xc}(\omega)$ has been proposed, which interpolates between high- and low-frequency limits.[10] At the large x-ray energies of interest here, this $f_{xc}(\omega)$ is strongly suppressed, and yields results close to the RPA.[6] However, such results are at odds with experiment for nearly empty d bands (Fig. 1).

(iv) Dynamic TDLDA/BSE model [cf. Eq. (4)]: Our aim in this paper is to improve on (i), (ii), and (iii) above, based partly on the BSE.[14–17] In the BSE, the matrix elements $\langle vc|f_{xc}(\omega)|v'c'\rangle$ depend on the nonlocal dynamically screened Coulomb interaction $W(\omega)=\tilde{\epsilon}^{-1}(\omega)V$, through an effective inverse dielectric matrix $\tilde{\epsilon}^{-1}(\omega)$.[16] However, the actual dependence on $\omega\approx E_c-E_v$ is matrix-element specific, and depends on the effective dielectric response at the energy-transfer frequency, i.e., $\tilde{\omega}=\omega+E_{c'}-E_v\approx E_{v'}-E_v$. This behavior can be seen explicitly in plasmon-pole models.[14] For $L_{2,3}$ XAS, the most important occupied states v,v' are the $2p_{1/2}$ and $2p_{3/2}$ levels, which are split by a moderate spin-orbit interaction Δ_{so}, ranging from 5 eV for Sc to 20 eV for Cu. The matrix elements with zero energy transfer correspond to static screening. Thus it is reasonable to set $f_{xc}(\omega)=f^0_{xc}$ for the diagonal terms $v=v'$.

For the off-diagonal elements ($v\neq v'$), we found that an unscreened exchange (i.e., the high-frequency limit $W\to V$ as in the TDHF model) has only a small effect [see (v) below]. These considerations suggest that the effects of dynamic screening on off-diagonal terms at moderately high frequency $\tilde{\omega}=\Delta_{so}$ are also small and can be neglected. This is in contrast to the case for optical absorption, where the adiabatic limit ($\tilde{\omega}=0$) is a good approximation for all matrix elements.[14] Thus, remarkably, we find that elaborate calculations of dynamical screening can be avoided for $L_{2,3}$ XAS by using a simplified dynamic TDLDA/BSE model $f_{xc}(\omega)\to\tilde{f}_{xc}(\tilde{\omega})$, $\tilde{\omega}=E_v-E_{v'}$ with matrix elements defined as follows:

$$\tilde{f}_{xc}(\tilde{\omega})=f^0_{xc} \quad (v=v';\tilde{\omega}=0)$$
$$=0 \quad (v\neq v';\tilde{\omega}=\Delta_{so}). \quad (4)$$

(v) The TDHF model: We also tried the unscreened, nonlocal TDHF exchange operator for $v=v'$ (which corresponds to an unscreened core-hole potential) but found it to be much too strong. For the off-diagonal elements ($v\neq v'$), however, we found that this unscreened exchange (i.e., the high-frequency limit $W\to V$) is quite small.

C. The TDLDA cross section

Next we briefly outline how the TDLDA is implemented in our calculations of the x-ray spectra. These calculations make use of the RSMS formalism (i.e., the real-space analog of the Koringa-Kohn Rostoker band-structure method) which is implanted in our self-consistent, FEFF8 code.[21] To begin, we rewrite Eq. (1) as

$$\sigma(\omega)=\frac{4\pi e^2\omega}{c}\sum_{v,LL'}\tilde{M}_{vL}(\omega)\rho_{L,L'}(E)\tilde{M}_{vL'}(\omega), \quad (5)$$

where $E=\omega+E_v-E_F$ is the photoelectron energy. Clearly, this representation of the TDLDA cross section separates the production and propagation parts of the problem. The photoelectron production is controlled by the renormalized dipole matrix elements $\tilde{M}_{vL}(\omega)=\langle R_L|\phi|v\rangle$, where $L=(\kappa,m)$ denotes a relativistic angular momentum basis. Note that the dielectric screening of both the x-ray field and the photoelectron–core-hole interaction can be included implicitly in the screened x-ray field ϕ.[19] The propagation is contained in $\rho_{L,L'}(E)=\mathrm{Im}\,G_{L,L'}(E)$, which is the imaginary part of the effective one-electron propagator $G(E)$. The quantities $\rho_{L,L'}(E)$ are matrix elements of the unoccupied one-electron spectral density matrix,

$$\rho(\vec{r},\vec{r},'E)\equiv\sum_c \psi_c(\vec{r})\psi^*_c(\vec{r}')\,\delta(E-E_c)$$
$$=\sum_{L,L'} R_L(\vec{r})R_{L'}(\vec{r}')\rho_{L,L'}(E),$$
$$\rho_{L,L'}(E)=\delta_{L,L'}+\chi_{L,L'}(E). \quad (6)$$

Here $R_L(\vec{r},E)$ are normalized scattering states calculated with the absorbing atom potential, and $\chi_{L,L'}(E)$ contains the fine structure due to scattering by the environment.[21] The above formalism emphasizes one of the advantages of our approach, since it can naturally treat both localized and extended states. In particular, it shows that the extended fine structure in the spectra is not substantially affected by the local screening of the smoothly varying dipole matrix elements.

Note that by replacing ϕ with ϕ^{ext} in Eq. (5), the screened matrix elements $\tilde{M}_{vL}$ become bare dipole matrix elements $M_{vL}=\langle R_L|\hat{\epsilon}\cdot\vec{r}|i\rangle$, and one recovers the independent-electron formula, equivalent to Fermi's golden rule. Since the strength of the XAS is a measure of the screening response, the independent-electron approximation should become increasingly valid away from the edge region.

D. Local screening approximation

Next we introduce a local embedded-atom basis to calculate the screening. One of the key approximations in our approach is the use of this basis for local calculations of χ_0 and $\tilde{M}_{vL}$. This is done starting from an expression for χ_0 in terms of a Kramers-Kronig (KK) transform over the density matrix,

$$\chi_0(\vec{r},\vec{r}',\omega)=\sum_v \psi_v^*(\vec{r})\psi_v(\vec{r}')\int_{E_F}^{\infty}\frac{dE}{\pi}\rho(\vec{r},\vec{r},'E) \times\left[\frac{1}{\omega-E+E_v+i\delta}+\frac{1}{\omega+E-E_v+i\delta}\right]. \quad (7)$$

Once χ_0 is known, Eq. (2) could be solved iteratively in real space to obtain $\phi(\vec{r})$.[2] However, this procedure is computationally expensive for extended systems, since it involves KK transforms for many $(\vec{r},\vec{r}',\omega)$ points. To simplify these calculations, we make the reasonable assumption that the induced charge $\rho^{ind}=\chi_0(\omega)\phi$ that screens the x-ray field is local[2] and arises largely from a few significant orbitals on the absorbing atom. This is convenient, since our formulation only needs the screened field $\phi(\vec{r},\omega)$ at short distances to calculate the deep-core transition matrix $\tilde{M}_{vL}(\omega)$. Thus to approximate ϕ, we introduce the atomic projection operator $P=\Sigma_n|\psi_n\rangle\langle\psi_n|$, which projects a given function onto a local basis set of atomiclike orbitals. Then the density matrix can be approximated by its local contribution $\rho\approx\rho^{loc}=P\rho P$. These approximations can be systematically improved by including a more complete set. Thus our local response function becomes

$$\chi_0^{loc}(\vec{r},\vec{r},'\omega)=\sum_{vnn'}\psi_v^*(\vec{r})\psi_n^*(\vec{r}')\chi^{loc}_{vn,vn'}(\omega)\psi_v(\vec{r}')\psi_{n'}(\vec{r}),$$

$$\chi^{loc}_{vn,vn'}(\omega)=-\frac{k}{\pi}\sum_{L,L'}\int_{E_F}^{\infty}dE\frac{\langle n|R_L\rangle\rho_{L,L'}\langle R_{L'}|n'\rangle}{\omega-E+E_v+i\delta}, \quad (8)$$

where $k=\sqrt{2(\omega+E_v)}$. Note that the localized part of χ_0 does not require a KK transform at each point, since the localized part of the photoelectron wave function can be separated into energy- and position-dependent parts. Moreover, the overlap matrices $\langle n|R_L\rangle$ decay rapidly with energy, so the KK transform converges well. This leads to a fast matrix formulation for $\tilde{M}_{vL}$.

From Eq. (2), we obtain

$$\phi(\vec{r},\omega)\approx\phi^{ext}(\vec{r},\omega)+\sum_{v'n'n''}\int d\vec{r}'K(\vec{r},\vec{r},'\omega) \times\psi_{v'}^*(\vec{r}')\psi_{n'}(\vec{r}')\chi^0_{v'n',v'n''}(\omega)\tilde{M}_{v'n''}, \quad (9)$$

where $\tilde{M}_{vn}=\langle\psi_n|\phi|v\rangle$ is calculated by integrating Eq. (9) over the core and basis set functions. Thus, summation over repeated indices being implicit,

$$\tilde{M}_{vn}(\omega)=M_{vn}+K_{vn,v'n'}\tilde{\chi}^{loc}_{v'n',v'n''}(\omega)\tilde{M}_{v'n''}(\omega),$$

$$M_{vn}=\langle n|\phi^{ext}|v\rangle, \quad (10)$$

$$K_{vn,v'n'}=\langle vn|K|v'n'\rangle.$$

These equations can readily be solved by matrix inversion. Finally, on integrating Eq. (9) over the core- and final-state wave functions, we get

$$\tilde{M}_{vL}(\omega)=M_{vL}(\omega)+K_{vL,v'n'}\chi^{loc}_{vn',v'n''}\tilde{M}_{v'n''},$$

$$M_{vl}(\omega)=\langle R_L|\phi^{ext}|v\rangle, \quad (11)$$

$$K_{vL,v'n'}=\langle vR_L|K|v'n'\rangle,$$

where R_L denotes the scattering state $R_L(\omega-E_v)$. The matrix elements $K_{vL,v'n'}$ satisfy the same selection rules and can be calculated using standard formulas for Coulomb matrix elements, i.e., the Slater term G_1.[24] The matrix form in Eq. (11) is very efficient, and has been implemented using an extension of our FEFF8 code. This extension is straightforward, since only the dipole matrix elements need to be modified to incorporate screening.

IV. COMPARISON WITH EXPERIMENT

A. Solid Xe

As a first example, we consider the case of $N_{4,5}$-edge XAS for solid Xe. As noted above, TDLDA calculations of XAS for atomic[2] Xe with a static kernel obtained from the ground-state LDA were remarkably successful in explaining the large deviations of the observed spectra from that calculated with the independent-electron approximation. The spectra for solid Xe, on the other hand, contain significant fine structure due to scattering from the environment,[25] which is straightforward to include within the real-space Green's-function approach considered here using Eq. (6).

Since these calculations involve x-ray energies of order 10^2 eV with only 2-eV spin-orbit splitting between $N_{4,5}$ edges, an adiabatic exchange-correlation kernel is reasonable. For the case of Xe, the final $4f$ states form a broad

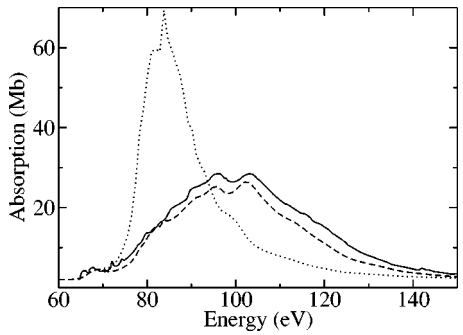

FIG. 2. $N_{4,5}$-edge XAS vs x-ray energy for solid Xe from experiment (solid),[25] and as calculated using the adiabatic TDLDA kernel $f_{xc}(0)$ (dashes) and with the independent particle approximation (dots).

scattering resonance with peak energy about 100 eV above the vacuum zero. To construct a local basis set that spans such continuum states, we have used the ''renormalized atom'' prescription.[26] Thus one confines an ''embedded'' atom within a finite sphere of volume equal to the volume per atom of solid Xe. This atomic sphere radius defines the Norman (or Wigner-Seitz) radius r_N, which is more convenient for heteroatomic materials. This prescription requires that the radial solution $R_L(r)$ has nodes at r_N. To cover the energy range of interest for Xe (i.e., 10–150 eV), we used four different orbitals of f character (energies 14.8, 31.5, 67.0, and 118.0 eV) and two orbitals of p character (energies 25.0 and 75.0 eV), and final-state spin-orbit interaction is neglected. With this choice of basis set, the matrix K is relatively large (78×78), and one needs to invert a matrix of the same size to calculate the screening. Thus the iterative calculation of self-consistent x-ray field in real space with the local kernel used by Zangwill and Soven is not necessarily slower computationally, since in their approach one has to calculate the field on a radial grid of about 200 points. However, for nonlocal exchange-correlation kernels (e.g., TDHF or BSE), the field $\phi(\vec{r},\vec{r}')$ is also nonlocal and hence requires a description as a matrix rather than a vector. In that case, our local projection method should be faster computationally, due to smaller matrix dimensions.

In Fig. 2, we show the results of N-shell calculations for Xe with the adiabatic kernel (ii), as well as the result from the independent-electron approximation ($\chi=\chi_0$ and $\phi=\phi^{ext}\equiv\hat{\epsilon}\cdot\vec{r}$). For comparison with the experimental Xe data,[25] we added a 2.0-Mb background to the calculated curves. As in the atomic calculations of Ref. 2, we also obtain better agreement with experiment for the adiabatic kernel. We also tried the RPA kernel, but found a much greater sensitivity to the neglect of exchange than in the atomic calculations.[2] One clearly sees that the experimental fine structure is also reasonably well reproduced. The remaining discrepancies are partially due to the finite basis set used in the screening calculations.

B. L-shell XAS for transition metals

Next we examine the results for L-shell XAS in transition metals. Typical results near the ends of the transition-metal series are presented for Ti and Ni in Fig. 3. For all calculations we used theoretical atomic core-hole lifetimes,[13] but no additional experimental broadening. Also we used a single atomic d orbital for the local screening calculations. The dramatic differences in the results reflect changes in the response between nearly empty and nearly filled d bands, and are strongly dependent on the form of $f_{xc}(\omega)$. From Eq. (8), for example, one sees that the response function should increase with the number of d holes, and hence screening effects are expected to be the largest for systems with small d counts. Clearly the RPA is only a good approximation for nearly empty d bands, while the adiabatic f_{xc}^0 is good only for nearly filled ones. Our results for the RPA agree well with those of Ref. 6, which validates our local screening approximation. However, our dynamic model $\tilde{f}_{xc}(\tilde{\omega})$ of Eq. (4) is clearly satisfactory for the entire series, and the spectral shape is improved compared to one-electron or RPA-TDLDA calculations.

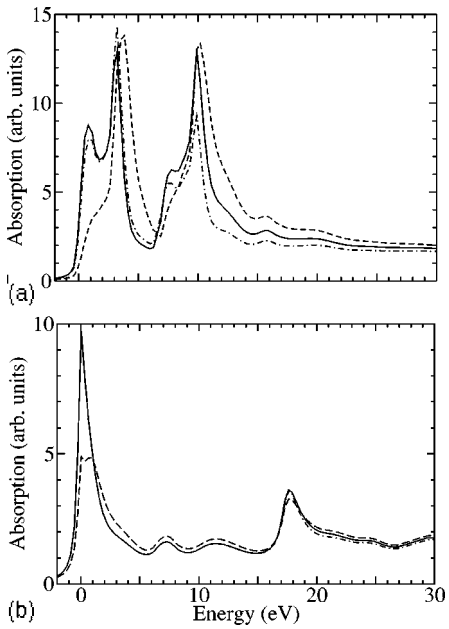

FIG. 3. $L_{3,2}$-edge XAS vs energy with respect to the Fermi level, for (a) Ti (upper figure) and (b) Ni (lower), calculated with different screening models: RPA (dashes), static fxc^0 (dash dots), and our dynamic model $\tilde{f}_{xc}(\omega)$ (solid).

We also carried out sample calculations for $4d$ and $5d$ elements, e.g., Y and W $L_{2,3}$ and $M_{2,3}$ spectra. For these cases the screening corrections turn out to be much smaller than those for $3d$ metals, and yield at most corrections of about 2%. This is consistent with the delocalized nature of $4d$ and $5d$ electrons, and hence the correspondingly smaller matrix elements of the Coulomb interaction kernel K.

Since screening redistributes the oscillator strength between the L_2 and L_3 edges, the validity of the ''sum rules'' for the spectra has been questioned.[6] Such sum rules allow one to determine various spin and orbital moments from linear combinations of the L_2 and L_3 XAS.[5,27] However with our approach, one can now correct these procedures for these local-field effects, e.g., by substituting the screened x-ray-absorption spectrum cross section, in place of the one-electron result in the analysis.

V. SUMMARY

In summary, we have developed a generalization of the TDLDA based partly on the BSE for including screening of the x-ray field and the core-hole interaction in x-ray-absorption spectrum calculations. The result for the XAS is analogous to that for independent-electron calculations based on golden rule, except that the dipole matrix elements are screened by the local dielectric response. In our approach, screening is calculated locally using a projection onto a local embedded atomic basis. Our approach includes continuum states within a real-space Green's-function approach and thus also can treat the fine structure in XAS.

We find that dynamic screening of the photoelectron–core-hole interaction is crucial in calculations of $3d$ transition-metal $L_{2,3}$ spectra. Moreover, we have shown that a simple dynamic exchange-correlation model based on the TDLDA and BSE accounts well for the frequency dependence of the matrix elements of this interaction. This approximation goes beyond the conventional TDLDA, and is similar to a screened TDHF approximation.[17] This approach has been implemented using a RSMS formalism that includes continuum states, and yields good agreement with experiment for the $L_{2,3}$ XAS of $3d$ transition metals, without the complexity of full dynamic-screening calculations. For $4d$ and $5d$ $L_{2,3}$ spectra, the screening corrections are much smaller than for $3d$, consistent with the less localized nature of $4d$ and $5d$ electrons. Our approach also accounts for the XAFS, and shows that the fine structure is not substantially affected by the screening.

Although extra-atomic screening is neglected in our model, it could be included in principle by extending the basis. Though local screening alone is justified in the cases considered here, extra-atomic screening can be important at frequencies for which the dielectric response of a neighboring atom is particularly strong.[28]

ACKNOWLEDGMENTS

We thank J. Chelikowsky, H. Ebert, W. Ku, Z. Levine, S. Pantelides, L. Reining, G. Sawatzky, E. Shirley and especially G. Bertsch and A. Soininen for helpful comments. We also thank L. Tröger for making available the experimental Xe data presented here. This work was supported by U.S. DOE Grants Nos. DE-FG03-97ER45623 and DE-FG03-98ER45718, and was facilitated by the U.S. DOE Computational Materials Science Network.

*Present address: Institute for Systems Biology, Seattle, WA 98103.

[1] J.J. Rehr and R.C. Albers, Rev. Mod. Phys. **72**, 621 (2000).
[2] A. Zangwill and P. Soven, Phys. Rev. A **21**, 1561 (1980); A. Zangwill and Liberman, J. Phys. B **17**, L253 (1984).
[3] J. Zaanen, G.A. Sawatzky, J. Fink, W. Speier, and J.C. Fuggle, Phys. Rev. B **32**, 4905 (1985).
[4] W.G. Waddington, P. Rez, I.P. Grant, and C.J. Humphreys, Phys. Rev. B **34**, 1467 (1986).
[5] B.T. Thole and G. van der Laan, Phys. Rev. B **38**, 3158 (1988).
[6] J. Schwitalla and H. Ebert, Phys. Rev. Lett. **80**, 4586 (1998).
[7] R.D. Leapman and L.A. Grunes, Phys. Rev. Lett. **45**, 397 (1980); R.D. Leapman, L.A. Grunes, and P.L. Fejes, Phys. Rev. B **26**, 614 (1982).
[8] J. Fink, Th. Müller-Heinzerling, B. Scheerer, W. Speier, F.U. Hillebrecht, J.C. Fuggle, J. Zaanen, and G.A. Sawatzky, Phys. Rev. B **32**, 4899 (1985).
[9] J. Barth, F. Gerken, and C. Kunz, Phys. Rev. B **28**, 3608 (1983).
[10] E.K.U. Gross, and W. Kohn, Adv. Quantum Chem. **21**, 255 (1990).
[11] I. Vasiliev, S. Ögut, and J. Chelikowsky, Phys. Rev. Lett. **82**, 1919 (1999).
[12] G.F. Bertsch, J.-I. Iwata, A. Rubio, and K. Yabana, Phys. Rev. B **62**, 7998 (2000).
[13] O. Keski-Rankonen and M.O. Krause, At. Data Nucl. Data Tables **14**, 139 (1974).
[14] M. Rohlfing and S.G. Louie, Phys. Rev. B **62**, 4927 (2000).
[15] J.A. Soininen and E.L. Shirley, Phys. Rev. B **64**, 165112 (2001).
[16] G. Strinati, Phys. Rev. B **29**, 5718 (1984).
[17] W. Hanke and L.J. Sham, Phys. Rev. B **21**, 4656 (1980).
[18] L. Reining, V. Olevano, A. Rubio, and G. Onida, Phys. Rev. Lett. **88**, 066404 (2002).
[19] Z. Crljen and G. Wendin, Phys. Rev. A **35**, 1555 (1987).
[20] B.I. Lundqvist, Phys. Kondens. Mater. **6**, 193 (1967).
[21] A.L. Ankudinov, B. Ravel, J.J. Rehr, and S.D. Conradson, Phys. Rev. B **58**, 7565 (1998).
[22] F. Aryasetiawan and O. Gunnarsson, Phys. Rev. Lett. **74**, 3221 (1995).
[23] M. Rohlfing, P. Krüger, and J. Pollmann, Phys. Rev. B **48**, 17 791 (1993).
[24] I.P. Grant, Adv. Phys. **19**, 747 (1970).
[25] L. Tröger (private communication); P. Schreiber, DESY internal Report No. DESY F41-70/5, 1970 (unpublished).
[26] L. Hodges, R.E. Watson, and H. Ehrenreich, Phys. Rev. B **10**, 3953 (1972).
[27] A.I. Nesvizhskii, A.L. Ankudinov, and J.J. Rehr, Phys. Rev. B **63**, 094412 (2001); A.L. Ankudinov, A.I. Nesvizhskii, and J.J. Rehr, J. Synchrotron Radiat. **8**, 92 (2001).
[28] F.J. Garcia de Abajo, M.A. Van Hove, and C.S. Fadley, Phys. Rev. B **63**, 075404 (2001).